

Architecture of Supramolecular Metal Complexes for Photocatalytic CO₂ Reduction: Ruthenium–Rhenium Bi- and Tetranuclear ComplexesBobak Gholamkhash,[†] Hiroaki Mametsuka,[‡] Kazuhide Koike,[§] Toyooki Tanabe,^{||} Masaaki Furue,^{||} and Osamu Ishitani^{*†}

Department of Chemistry, Graduate School of Science and Engineering, Tokyo Institute of Technology, 2-12-1 Okayama, Meguro-ku, Tokyo 152-8551, Japan, CREST, Japan Science and Technology Corporation, Research Institute of Innovative Technology for the Earth, 9-2 Kizugawa-dai, Kizu-cho, Sorakugun, Kyoto 619-0292, Japan, National Institute of Advanced Industrial Science and Technology, 16-1 Onogawa, Tsukuba West, Ibaraki 305-8569, Japan, and Department of Environmental Systems Engineering, Kochi University of Technology, 185 Miyanokuchi, Tosayamada-cho, Kamigun, Kochi 782-8502, Japan

Received September 1, 2004

We study the electrochemical, spectroscopic, and photocatalytic properties of a series of Ru(II)–Re(I) binuclear complexes linked by bridging ligands 1,3-bis(4'-methyl-[2,2']bipyridinyl-4-yl)propan-2-ol (bpyC₃bpy) and 4-methyl-4'-[1,10]phenanthroline-[5,6-d]imidazol-2-yl)bipyridine (mfibpy) and a tetranuclear complex in which three [Re(CO)₃Cl] moieties are coordinated to the central Ru using the bpyC₃bpy ligands. In the bpyC₃bpy binuclear complexes, 4,4'-dimethyl-2,2'-bipyridine (dmb) and 4,4'-bis(trifluoromethyl)-2,2'-bipyridine ({CF₃})₂bpy), as well as 2,2'-bipyridine (bpy), were used as peripheral ligands on the Ru moiety. Greatly improved photocatalytic activities were obtained only in the cases of [Ru{bpyC₃bpyRe(CO)₃Cl}]₃²⁺ (**RuRe₃**) and the binuclear complex [(dmb)₂Ru(bpyC₃bpy)Re(CO)₃Cl]²⁺ (**d₂Ru–Re**), while photocatalytic responses were extended further into the visible region. The excited state of ruthenium in all Ru–Re complexes was efficiently quenched by 1-benzyl-1,4-dihydronicotinamide (BNAH). Following reductive quenching in the case of **d₂Ru–Re**, generation of the one-electron-reduced (OER) species, for which the added electron resides on the Ru-bound bpy end of the bridging ligand bpyC₃bpy, was confirmed by transient absorption spectroscopy. The reduced Re moiety was produced via a relatively slow intramolecular electron transfer, from the reduced Ru-bound bpy to the Re site, occurring at an exchange rate ($\Delta G \sim 0$). Electron transfer need not be rapid, since the rate-determining process is reduction of CO₂ with the OER species of the Re site. Comparison of these results with those for other bimetallic systems gives us more general architectural pointers for constructing supramolecular photocatalysts for CO₂ reduction.

Introduction

Multinuclear metal complexes play a central role in the study of supramolecular structures as possible building blocks for photochemical and electrochemical molecular assemblies.¹ Many multinuclear compounds containing two or more

metallic sites have been synthesized, and their optical, electronic, and photophysical properties have been studied.^{1,2} In particular, ruthenium and rhenium polypyridine complexes are popular in both fundamental studies and applications.^{3,4} These complexes form appealing subunits for nanoscaled

* Author to whom correspondence should be addressed. E-mail: ishitani@chem.titech.ac.jp.

[†] Tokyo Institute of Technology.

[‡] Research Institute of Innovative Technology for the Earth.

[§] National Institute of Advanced Industrial Science and Technology.

^{||} Kochi Institute of Technology.

(1) (a) Steed, J. W.; Atwood, J. L. *Supramolecular Chemistry*; John Wiley & Sons: West Sussex, U.K., 2000. (b) Sauvage, J.-P. *Transition Metals in Supramolecular Chemistry*; John Wiley & Sons: West Sussex, U.K., 1999; Vol. 5. (c) Lehn, J.-M. *Supramolecular Chemistry*; VCH: Weinheim, Germany, 1995.

(2) (a) Balzani, V.; Juris, A.; Venturi, M.; Campagna, S.; Serroni, S. *Chem. Rev.* **1996**, *96*, 759. (b) Scandola, F.; Indelli, M. T.; Chiorboli, C.; Bignozzi, C. A. *Top. Curr. Chem.* **1990**, *158*, 73. (c) Bardwell, D. A.; Barigelletti, F.; Cleary, R. L.; Flamigni, L.; Guardigli, M.; Jeffery, J. C.; Ward, M. D. *Inorg. Chem.* **1995**, *34*, 2438. (d) Gholamkhash, B.; Nozaki, N.; Ohno, T. *J. Phys. Chem. B* **1997**, *101*(44), 9010. (e) Warnmark, K.; Thomas, J. A.; Heyke, O.; Lehn, J.-M. *Chem. Commun.* **1996**, 701. (f) Argazzi, R.; Bignozzi, C. A.; Heimer, T. A.; Meyer, G. *J. Inorg. Chem.* **1997**, *36*, 2.

(3) (a) Meyer, T. J. *Pure Appl. Chem.* **1986**, *58*, 1193. (b) Juris, A.; Balzani, V.; Barigelletti, F.; Campagna, S.; Belsler, P.; von Zelewsky, A. *Coord. Chem. Rev.* **1988**, *84*, 85.

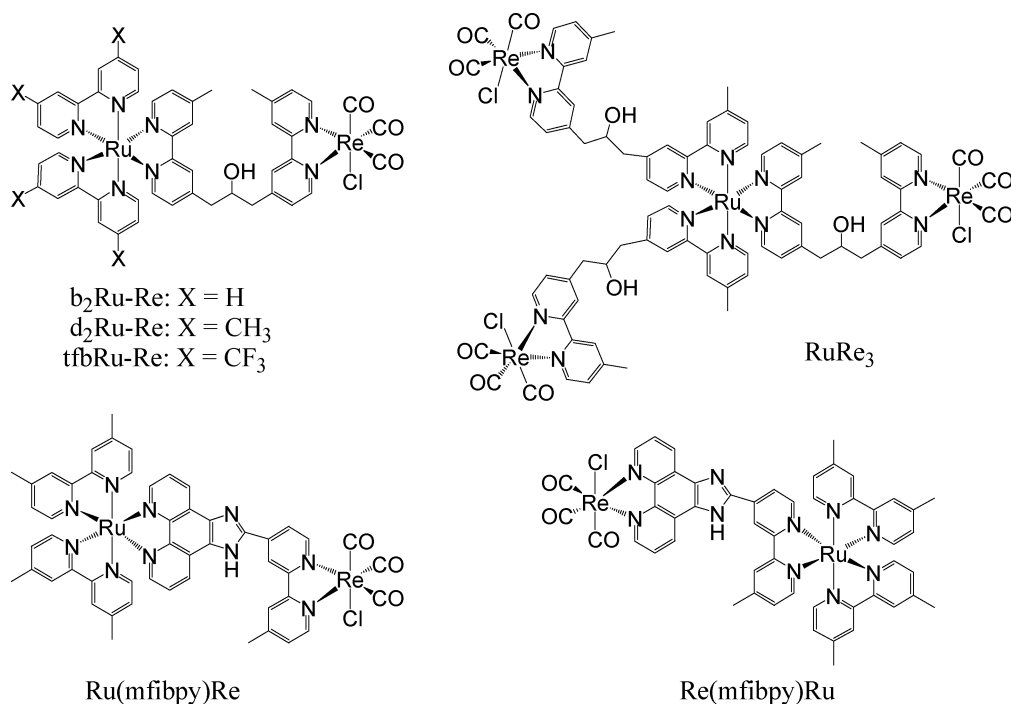


Figure 1. Schematic representation of the metal complexes and their abbreviations.

devices⁵ because of their strong visible absorption, their advanced photochemical and redox properties, and their stability against photodecomposition.⁶ There exist a number of means to fine-tune these features via made-to-order modifications on peripheral ligands.⁷ Rhenium polypyridine complexes are known to act as photocatalysts and electrocatalysts for reducing CO₂ to CO.⁸ A major problem with these photocatalysts is the lack of an extended absorption into the visible region. The present approach is to fabricate supramolecules of the rhenium complex linked covalently to the ruthenium complex as a visible-light absorber. We believe that this is the first report of the use of heteronuclear Ru and Re multimetallic complexes in the photocatalytic reduction of CO₂.⁹

Although some examples of mononuclear¹⁰ and multinuclear¹¹ photocatalysts, such as Ru(II)–Co(III)^{11a} and Ru(II)–Ni(II),^{11d} have appeared in the literature, their activities for CO₂ reduction are not satisfactory. Although a mechanistic approach has been tried,¹⁰ the controlling parameters that define structural requirements and electrochemical properties, which are essential in the design of new supramolecular photocatalysts, have not yet been systematically investigated. This study therefore aims also to learn how photocatalytic properties can be related to, and manipulated by, structural changes in such supramolecules. We are particularly interested in the assembly of multinuclear complexes involving different degrees of electronic communication between the metallic sites and “tunable” polypyridine ligands.

In this study, we describe the electrochemical, spectroscopic, and photocatalytic properties of a series of Ru(II)–Re(I) binuclear complexes linked by the bridging ligands (i) 1,3-bis(4'-methyl-[2,2']bipyridinyl-4-yl)propan-2-ol (bpyC₃-bpy)¹² and (ii) 4-methyl-4'-[1,10]phenanthroline-[5,6-*d*]imi-

dazol-2-yl)bipyridine (mfibpy) and a tetranuclear complex **Ru(Re)₃** in which three [Re(CO)₃Cl] moieties are coordinated to the central Ru using the bpyC₃bpy ligands. Their structures are shown in Figure 1. In the case of the bpyC₃bpy complexes, a number of substituted bpy ligands, i.e., 4,4'-dimethyl-2,2'-bipyridine (dmb) and 4,4'-bis(trifluoromethyl)-2,2'-bipyridine ({CF₃}₂bpy), as well as 2,2'-bipyridine (bpy)

- (4) (a) Splan, K. E.; Keefe, M. H.; Massari, A. M.; Walters, K. A.; Hupp, J. T. *Inorg. Chem.* **2002**, *41*, 619. (b) Constable, E. C.; Schofield, E. *Chem. Commun.* **1998**, 403. (c) Fujita, M. *Chem. Soc. Rev.* **1998**, *27*, 417.
- (5) Dagani, R. *Chem. Eng. News* **2000**, *78* (1), 22–26.
- (6) Kalyanasundaram, K. *Photochemistry of Polypyridine and Porphyrin Complexes*; Academic Press Inc.: San Diego, CA, 1992.
- (7) Furue, M.; Ishibashi, M.; Satoh, A.; Oguni, T.; Maruyama, K.; Sumi, K.; Kamachi, M. *Coord. Chem. Rev.* **2000**, *208*, 103.
- (8) (a) Hawecker, J.; Lehn, J.-M.; Ziessel, R. *J. Chem. Soc., Chem. Commun.* **1983**, 536. (b) Hawecker, J.; Lehn, J.-M.; Ziessel, R. *Helv. Chim. Acta* **1986**, *69*, 1990. (c) Koike, K.; Hori, H.; Ishizuka, M.; Westwell, J. R.; Takeuchi, K.; Ibusuki, T.; Enjouji, K.; Konno, H.; Sakamoto, K.; Ishitani, O. *Organometallics* **1997**, *16*, 5724. (d) Hori, H.; Johnson, F. P. A.; Koike, K.; Ishitani, O.; Ibusuki, T. *J. Photochem. Photobiol. A: Chem.* **1996**, *96*, 171.
- (9) (a) Argazzi, R.; Bignozzi, C. A.; Heimer, T. A.; Meyer, G. J. *Inorg. Chem.* **1997**, *36*, 2. (b) Argazzi, R.; Bignozzi, C. A.; Bortolini, O.; Traldi, P. *Inorg. Chem.* **1993**, *32*, 1222. (c) van Wallendaal, S.; Perkovic, M. W.; Rillema, D. P.; *Inorg. Chim. Acta* **1993**, *213*, 253. (d) Schoonover, J. R.; Gordon, K. C.; Argazzi, R.; Woodruff, W. H.; Peterson, K. A.; Bignozzi, C. A.; Dyer, R. B.; Meyer, T. J. *J. Am. Chem. Soc.* **1993**, *115*, 10996.
- (10) (a) Ogata, T.; Yanagida, S.; Brunschwig, B. S.; Fujita, E. *J. Am. Chem. Soc.* **1995**, *117*, 6708. (b) Ooyama, D.; Tomon, T.; Tsuge, K.; Tanaka, K. *J. Organomet. Chem.* **2001**, *619*, 299. (c) Nakajima, H.; Kushi, Y.; Nagao, H.; Tanaka, K. *Organometallics* **1995**, *14*, 5093.
- (11) (a) Komatsuzaki, N.; Himeda, Y.; Takeuji, H.; Sugihara, H.; Kasuga, K. *Bull. Chem. Soc. Jpn.* **1999**, *72*, 725. (b) Kimura, E.; Bu, X.; Shionoya, M.; Wada, S.; Maruyama, S. *Inorg. Chem.* **1992**, *31*, 4542. (c) Kimura, E.; Haruta, M.; Koike, T.; Shionoya, M.; Takenouchi, K.; Itaka, Y. *Inorg. Chem.* **1993**, *32*, 2779. (d) Kimura, E.; Bu, X.; Shionoya, M.; Wada, S.; Maruyama, S. *Inorg. Chem.* **1994**, *33*, 770. (e) Mochizuki, K.; Manaka, S.; Takeda, I.; Kondo, T. *Inorg. Chem.* **1996**, *35*, 5132.
- (12) Furue, M.; Naiki, M.; Kanematsu, Y.; Kushida, T.; Kamachi, M. *Coord. Chem. Rev.* **1991**, *111*, 221.

itself, were used as peripheral ligands so as to fine-tune the electrochemical and photochemical properties of the supramolecular complexes.

Experimental Section

Instrumentation and Measurements. Absorption spectra were measured on a JASCO V-565 spectrophotometer. Emission spectra were recorded with a JASCO FP-6600 spectrofluorometer. These spectra were corrected for detector sensitivity using correction data supplied by JASCO on the FP-6600 system, and a single-mode Franck–Condon line-shape analysis was used to fit the emission spectra.^{13a,b} The solutions were bubble degassed for 20 min with purified argon prior to measurements. Emission lifetimes of the metal complexes were measured with either a Horiba NAES-1100 time-correlated single-photon-counting system or a Continuum YG680-10 Nd³⁺:YAG pulse laser source, as described previously.^{13c} Nanosecond laser spectroscopy was employed to measure the transient absorption spectra and corresponding lifetimes.^{13c}

Luminescence quenching experiments were made on argon-saturated solutions of at least five different concentrations of a sacrificial quencher. The values of k_q were calculated from linear Stern–Volmer plots for the luminescence of Ru ³MLCT excited state and knowledge of its lifetime.

Electrospray ionization–mass spectroscopy (ESI-MS) was performed with a Shimadzu LCMS-2010A system, using HPLC-grade acetonitrile (MeCN) or CH₃OH/H₂O (1:1) as the mobile phase.

Redox potentials of metal complexes were measured by cyclic and differential-pulse voltammetry using an ALS/CHI CHI620 electrochemical analyzer in a standard three-cell electrode arrangement. Voltammograms were recorded using a platinum working electrode (diameter, 2 mm) in MeCN or a glassy-carbon (3 mm) in dimethylformamide (DMF) solutions of the complexes containing 0.1 M supporting electrolyte, tetra-*n*-butylammonium hexafluorophosphate (TBAH).

Photocatalytic reduction was performed in a 10-mL test tube (i.d. = 1 cm) containing 4 mL DMF/TEOA (5:1) solution of the metal complexes (0.05 mM) and a sacrificial reagent (0.1 M) after purging with CO₂ for 20 min. For a selective excitation of the ruthenium moiety, solutions were irradiated at $\lambda \geq 500$ nm using a high-pressure Hg lamp, in a merry-go-round irradiation apparatus, combined with a uranyl glass and a K₂CrO₄ (30% w, $d = 1$ cm) solution filter. For the quantum yield measurements, an Ushio (Optical Modulex) Xe lamp SX-U1500H combined with a 480 nm (fwhm = 10 nm) band-pass filter, purchased from Asahi Spectra Co., and a 10-cm long CuSO₄ solution (250 g/L) filter were used. All experiments were conducted at the ambient temperature. Gas samples were taken using a gastight syringe. The gaseous reaction products, i.e., CO and H₂, were detected by GC-TCD. The incident light intensity was determined using a K₃Fe(C₂O₄)₃ actinometer. Formation of organic acids was checked by capillary electrophoresis system (CAPI-3300I Photal, Otsuka Electronics).

Materials. MeCN was purified by fractional distillation from P₂O₅ after having been dried for 1 day over 4 Å molecular sieves followed by distillation over CaH₂. DMF was dried over 4 Å molecular sieves and distilled at reduced pressure. Triethanolamine (TEOA) was also distilled at reduced pressure. All of the purified solvents were kept under Ar before use. The spectroscopic data

were obtained on samples dissolved in the purified or spectral-grade solvents. Hydrated ruthenium trichloride was purchased from Kojima Chemical Co. and used as received. TBAH (Tokyo Kasei) was recrystallized from ethanol (EtOH). All other reagents were reagent-grade quality and were used without further purification.

Synthesis. 1-Benzyl-1,4-dihydrocinotinamide (BNAH),¹⁴ 1,10-phenanthroline-5,6-dione (phenO₂),¹⁵ [Ru(dmb)₂Cl₂] \cdot 2H₂O,¹⁶ and [Ru(DMSO)₄Cl₂]¹⁷ were prepared according to the literature methods. 4-Methyl-2,2'-bipyridine-4'-carboxaldehyde (Mebpy-CHO),¹⁸ 4,4'-bis(trifluoromethyl)-2,2'-bipyridine (CF₃)₂bpy, [((CF₃)₂bpy)₂RuCl₂],¹⁹ and [(bpy)₂Ru(bpyC₃bpy)Re(CO)₃Cl](PF₆)₂, **b₂Ru–Re**,¹² were prepared as described previously. The synthesis and purification methods used for mfibpy and its mononuclear and binuclear complexes as well as the Ru(Re)₃ tetranuclear species are described below. All complexes were characterized by ¹H NMR, ESI-MS, FTIR, absorption, and emission spectroscopies.

(a) [((CF₃)₂bpy)₂Ru(bpyC₃bpy)](CF₃SO₃)₂. To a solution of bpyC₃bpy (900 mg, 2.27 mmol) in 50 mL of MeOH/H₂O (9:1) was added [((CF₃)₂bpy)₂RuCl₂] (340 mg, 0.45 mmol) and AgCF₃SO₃ (250 mg, 0.97 mmol), and the argon-purged mixture was heated at reflux for 7 h under argon in dark condition. The reaction mixture was filtered over Celite while hot. The filtrate was concentrated to few milliliters and subjected to Sephadex LH20 chromatography, using MeOH as eluent. The product was precipitated from the concentrate by addition of water, filtered out and washed thoroughly with water, and vacuum-dried. Yield: 71%, 440 mg. Anal. Calcd for C₅₁H₃₆F₁₈N₈O₇RuS₂: C, 43.65; H, 2.77; N, 7.98. Found: C, 43.67; H, 2.80; N, 8.04. ESI-MS in MeCN (m/z): 541, [M – 2CF₃SO₃]²⁺. ¹H NMR [CD₃CN] [δ in ppm (integration, multiplicity), assignment]: 2.51 (6H, s), methyl; 2.8–3.1 (4H, m), methylene; 3.18 (1H, br), OH; 4.26 (1H, br), methyne; 7.2–8.9 (24H, m), bpy ring protons.

(b) [((CF₃)₂bpy)₂Ru(bpyC₃bpy)Re(CO)₃Cl](PF₆)₂, **tfbRu–Re**. The binuclear complex was prepared by reacting [((CF₃)₂bpy)₂Ru(bpyC₃bpy)](CF₃SO₃)₂ (100 mg) and Re(CO)₃Cl (30 mg) in 40 mL of MeOH for 35 h. After this period, the concentrate was subjected to Sephadex LH20 chromatography, using MeOH as eluent. The product was precipitated from the concentrate by addition of an aqueous solution of NH₄PF₆, filtered out and washed with water, and vacuum-dried. Yield: 91%, 110 mg. Anal. Calcd for C₅₂H₃₆ClF₂₄N₈O₄P₂ReRu: C, 37.23; H, 2.16; N, 6.68. Found: C, 37.21; H, 2.42; N, 6.46. ESI-MS in MeCN (m/z): 694, [M – 2PF₆]²⁺; 1533, [M – PF₆]⁺.

(c) [(dmb)₂Ru(bpyC₃bpy)Re(CO)₃Cl](PF₆)₂, **d₂Ru–Re**. The binuclear complex was prepared by the method described for [(bpy)₂Ru(bpyC₃bpy)Re(CO)₃Cl](PF₆)₂.¹² Briefly, [(dmb)₂Ru(bpyC₃bpy)]Cl₂ (70 mg) and Re(CO)₃Cl (28 mg) were reacted in 100 mL of 1,2-dichloroethane for 3 h. After this period, the product was precipitated from the concentrate by addition of NH₄PF₆(aq), filtered out, and washed with water. The crude was subjected to column chromatography on SP Sephadex C-25 using a 1:1 mixture of MeCN and aqueous buffer (pH 5.0, containing 20 mM NH₄PF₆) as eluant, followed by precipitation of the product from the concentrate and filtration. The product was dissolved in 50 mL of

(13) (a) Worl, L. A.; Duesing, R.; Chen, P.; Della Ciana, L.; Meyer, T. J. *J. Chem. Soc., Dalton Trans.* **1991**, 849. (b) Caspar, J. V.; Kober, E. M.; Sullivan, B. P.; Meyer, T. J. *J. Am. Chem. Soc.* **1982**, *104*, 630. (c) Gholamkhash, B.; Koike, K.; Negishi, N.; Hori, H.; Sano, T.; Takeuchi, K. *Inorg. Chem.* **2003**, *42*, 2919.

(14) Schanze, K. S.; Lee, L. Y. C.; Giannotti, C.; Whitten, D. G. *J. Am. Chem. Soc.* **1986**, *108*, 2646.
(15) Amouyal, E.; Homsy, A.; Chambron, J.-C.; Sauvage, J.-P. *J. Chem. Soc., Dalton Trans.* **1990**, 1841.
(16) Sullivan, B. P.; Meyer, T. J. *Inorg. Chem.* **1978**, *17*, 3334.
(17) Goss, C. A.; Abruna, H. D. *Inorg. Chem.* **1985**, *24*, 4263.
(18) Furue, M.; Yoshidzumi, T.; Kinoshita, S.; Kushida, T.; Nozakura, S.; Kamachi, M. *Bull. Chem. Soc. Jpn.* **1991**, *64*, 1632.
(19) Furue, M.; Maruyama, K.; Oguni, T.; Naiki, M.; Kamachi, M. *Inorg. Chem.* **1992**, *31*, 3792.

acetone/H₂O (1:1) containing 0.1 M NH₄Cl and heated at reflux condition for 30 min. The product was reprecipitated from the concentrate by addition of an aqueous solution of NH₄PF₆, filtered out and washed with water, and vacuum-dried. Yield: 90%, 95 mg. Anal. Calcd for C₅₂H₄₈ClF₁₂N₈O₄P₂ReRu: C, 42.73; H, 3.31; N, 7.67. Found: C, 42.45; H, 3.61; N, 7.41. ESI-MS in MeCN (*m/z*): 586, [M – 2PF₆]²⁺; 1317, [M – PF₆]⁺.

(d) 4-Methyl-4'-[1,10]phenanthroline-[5,6-*d*]imidazol-2-yl)-bipyridine, mfibpy. A portion of 96 mg (0.46 mmol) of phenO₂ in hot EtOH (25 mL) was added to a mixture of 90 mg (0.46 mmol) of MebpyCHO and 0.5 g of ammonium acetate in 25 mL of EtOH. The mixture was allowed to reflux for 3 h and then cooled. The volume of the reaction was reduced to ca. 5 mL by rotary evaporation. After addition of water to the concentrate, a yellow precipitate was formed. The crude product was filtered out and washed with water. It was recrystallized from a mixture of EtOH and water. Yield: 51%, 90 mg. Anal. Calcd for C₂₄H₁₆N₆: C, 74.21; H, 4.15; N, 21.64. Found: C, 74.48; H, 4.08; N, 21.42.

(e) [(MebpyCHO)Re(CO)₃Cl]. A mixture of [Re(CO)₅Cl] (150 mg, 0.41 mmol) and MebpyCHO (82 mg, 0.41 mmol) in 100 mL of argon-purged toluene was refluxed for 3 h. The reaction mixture turned red within few minutes, and an orange-red precipitate was gradually formed. It was then cooled, and the orange precipitate was filtered off, washed with toluene and hexane, and vacuum-dried. Yield: 95%, 198 mg. Anal. Calcd for C₁₅H₁₀ClN₂O₄Re: C, 35.75; H, 2.00; N, 5.56. Found: C, 35.99; H, 1.98; N, 5.44. ¹H NMR (CD₃CN) [δ in ppm (integration, multiplicity), assignment]: 10.17 (1H, s), CHO; 9.26 (1H, d), 6'; 8.86 (1H, d), 6; 8.78 (1H, s), 3'; 8.44 (1H, s), 3; 7.97 (1H, dd), 5'; 7.51 (1H, dd), 5; 2.59 (3H, s), methyl.

(f) [(mfibpy)Re(CO)₃Cl]. To a mixture of 60 mg (0.12 mmol) of [(MebpyCHO)Re(CO)₃Cl] and 0.5 g of ammonium acetate in 25 mL of EtOH was added 40 mg (0.19 mmol) of phenO₂ dissolved in hot EtOH (25 mL). The mixture was allowed to reflux for 3 h and then was cooled. The volume of the reaction was reduced to ca. 5 mL by rotary evaporation. After addition of water to the concentrate, a brown precipitate was formed. The crude product was filtered out and washed with water. It was recrystallized from acetone and vacuum-dried. Yield: 93%, 77 mg. Anal. Calcd for C₂₇H₁₆ClN₆O₃Re·CH₃COCH₃: C, 47.90; H, 2.95; N, 11.17. Found: C, 47.93; H, 2.84; N, 10.82. ESI-MS in MeCN (*m/z*): 700.9, [M – Cl + MeCN]⁺. ¹H NMR (CD₃CN) [δ in ppm (integration, multiplicity), assignment]: 9.27 (1H, d), c'; 9.23 (1H, dd), a'; 9.21 (1H, dd), 6'; 9.13 (1H, s), 3'; 8.93 (1H, d), c; 8.89 (1H, dd) a; 8.78 (1H, dd), 6; 8.57 (1H, s), 3; 8.10 (2H, m), 4'; 7.98 (2H, m), 4; 7.86 (1H, dd), b'; 7.78 (1H, dd), b; 7.83 (2H, dd), 6'; 8.35 (1H, dd), b'; 7.94 (1H, dd), 5'; 7.90 (1H, dd), b; 7.51 (1H, dd), 5; 2.64 (3H, s), methyl.

(g) [(dmb)₂Ru(mfibpy)Re(CO)₃Cl](PF₆)₂, Ru(mfibpy)Re. [(mfibpy)Re(CO)₃Cl] (35 mg) and [Ru(dmb)₂Cl₂]·2H₂O (28 mg) were allowed to react in argon-purged ethylene glycol (5 mL) at 150 °C. After 1 h, the reaction mixture was cooled to room temperature, and the product was precipitated by addition of an aqueous solution of NH₄PF₆ (15 mL). The orange precipitate was filtered off, washed with water, and recrystallized by slow evaporation of acetone from an aqueous solution. The product can further be purified by column chromatography on SP Sephadex C-25 using a 1:1 mixture of MeCN and aqueous buffer (pH 5.0, containing 20 mM NH₄PF₆) as eluant, followed by precipitation of the product from the concentrate by adding NH₄PF₆(aq) and recrystallization in EtOH/H₂O. Yield: 36%, 26 mg. Anal. Calcd for C₅₁H₄₀F₁₂-ClN₁₀O₃P₂ReRu: C, 42.14; H, 2.77; N, 9.64. Found: C, 42.44; H,

3.04; N, 9.86. ESI-MS in MeCN (sample dissolved in acetone) (*m/z*): 582, [M – 2PF₆]²⁺; 612, [M – 2PF₆ + CH₃COCH₃]²⁺.

(h) [(dmb)₂Ru(MebpyCHO)](PF₆)₂. A mixture of [Ru(dmb)₂Cl₂]·2H₂O (68 mg, 0.12 mmol) and MebpyCHO (30 mg, 0.15 mmol) in 50 mL of EtOH/H₂O (4:1) was refluxed for 7 h. The solution was then cooled to room temperature and concentrated. A saturated solution of NH₄PF₆ in water was added to the concentrate. The orange precipitate was filtered off and washed with cold water. The product was subjected to column chromatography on SP Sephadex C-25 using a 1:1 mixture of MeCN and aqueous buffer (pH 5.0) as eluant. A center cut of the orange band was collected. A saturated solution of NH₄PF₆ in H₂O was again added to the concentrate, and the precipitate was recrystallized from MeOH/H₂O. Yield: 62%, 70 mg. Anal. Calcd for C₃₆H₃₄F₁₂N₆OP₂Ru: C, 45.15; H, 3.58; N, 8.78. Found: C, 45.12; H, 3.84; N, 8.48. ESI-MS in MeCN (*m/z*): 334, [M – 2PF₆]²⁺; 813, [M – PF₆]⁺.

(i) [(mfibpy)Ru(dmb)₂](PF₆)₂, (mfibpy)Ru. A mixture of [Ru(dmb)₂Cl₂]·2H₂O (40 mg, 0.07 mmol) and mfibpy (40 mg, 0.07 mmol) in 50 mL of EtOH/H₂O (4:1) was refluxed for 4 h. The reaction mixture was cooled and concentrated by rotary evaporation. A saturated solution of NH₄PF₆ in water was added to the concentrate, and the orange precipitate that formed was filtered off and washed with water. The product was subjected to column chromatography on SP Sephadex C-25 using a 1:1 mixture of MeCN and aqueous buffer (pH 5.0) as eluant. A center cut of the first orange band was collected. The second orange-red band is the binuclear complex, [(dmb)₂Ru(mfibpy)Ru(dmb)₂](PF₆)₄, and can be eluted by increasing concentration of NH₄PF₆ in the buffer. A saturated solution of NH₄PF₆ in H₂O was again added to the concentrate, and the precipitate was recrystallized from MeOH/H₂O. Yield: 54%, 43 mg. Anal. Calcd for C₄₈H₄₀F₁₂N₁₀P₂Ru: C, 50.22; H, 3.51; N, 12.20. Found: C, 49.95; H, 3.77; N, 11.91. ESI-MS in MeCN (*m/z*): 429, [M – 2PF₆]²⁺; 857, [M – 2PF₆ – H]⁺; 1003, [M – PF₆]⁺. ¹H NMR (acetone-*d*₆) [δ in ppm (integration, multiplicity), assignment]: 9.19 (1H, s), 3'''; 8.92 (2H, d), aa'; 8.66 (1H, d), 6'''; 8.62 (1H, d), c'; 8.40 (2H, s), 3'; 8.37 (2+1H, s), 3 and c; 8.32 (1H, s), 3''; 8.01 (2H, dd), bb'; 7.66 (3H, d), 6' and 6''; 7.57 (1H, d), 5'''; 7.46 (2H, d), 6; 7.30 (2H, d), 5'; 7.25 (1H, d), 5''; 7.09 (2H, d), 5; 2.58 (6H, s), 2.56 (3H, s) and 2.48 (6H, s), methyls.

(j) [Cl(CO)₃Re(mfibpy)Ru(dmb)₂](PF₆)₂, Re(mfibpy)Ru. [(mfibpy)Ru(dmb)₂](PF₆)₂ (25 mg) and [Re(CO)₃Cl] (8 mg) were allowed to react in argon-purged ethylene glycol (3 mL) at 160 °C. After 10 min, the reaction mixture was cooled to room temperature, and the product was precipitated by addition of an aqueous solution of NH₄PF₆ (15 mL). The brown precipitate was filtered off and washed with water. The crude was purified by column chromatography on SP Sephadex C-25 using a 1:1 mixture of MeCN and aqueous buffer (pH 5.0, containing 10 mM NH₄PF₆) as eluant, followed by precipitation of the product from the concentrate by adding NH₄PF₆(aq). The recrystallization performed in MeCN/MeOH/NH₄PF₆(aq). Yield: 50%, 15.4 mg. Anal. Calcd for C₅₁H₄₀F₁₂ClN₁₀O₃P₂ReRu: C, 42.14; H, 2.77; N, 9.64. Found: C, 42.08; H, 2.99; N, 9.47. ESI-MS in MeCN (*m/z*): 582, [M – 2PF₆]²⁺.

(k) [Ru{bpyC₃bpyRe(CO)₃Cl}₃](PF₆)₂, RuRe₃. Ru(DMSO)₄-Cl₂ (407 mg) and bpyC₃bpy (1 g) were allowed to react in EtOH/H₂O (50:1) at reflux condition for 48 h. Then the solvent was evaporated and the residue was subjected to column chromatography on Sephadex LH-20 using EtOH as solvent which gave analytically pure Ru(bpyC₃bpy)₃Cl₂ (yield 59%, 680 mg). The resulted complex Ru(bpyC₃bpy)₃Cl₂ (50 mg) and Re(CO)₃Cl (46 mg) were allowed to react in argon-purged EtOH/DMF (50:10) at reflux. After 24 h,

Table 1. Turnover Number (TN_{CO}), CO Production Yields (Φ_{CO}), and Quenching Rate (k_q) and Fractions (η_q)

compd	TN _{CO} ^a	Φ _{CO} ^b	10 ⁻⁸ k _q ^c /M ⁻¹ s ⁻¹	η _q ^d
mixed Ru and Re (1:1) ^e	101	0.062	0.26	0.71
d ₂ Ru–Re	170	0.120	1.4	0.90
b ₂ Ru–Re	50 ^f		2.3	0.95
tfbRu–Re	3		61	~1.0
Ru(mfibpy)Re	14		0.75	0.8
Re(mfibpy)Ru	28 ^g		1.5	0.95
RuRe ₃	240	0.093	2.8	0.96

^a TN_{CO} is the turnover number for production of CO following 16 h of irradiation; [complex] = 0.05 mM. ^b The best value obtained following 40 min irradiation at 480 nm ($I = 1.54 \times 10^{-6}$ einstein/min) in CO₂-saturated solutions. ^c The values were obtained at room temperature and in N₂-saturated DMF/TEOA (5:1) solutions containing metal complexes and BNAH as the sacrificial reagent. In the calculation of k_q, the excited-state lifetimes measured in MeCN were applied. ^d Quenching fractions of ³MLCT by 0.1 M BNAH. ^e Mixed solution of [Ru(dmb)₃]²⁺ and [(dmb)Re(CO)₃Cl]. ^f After 12.5 h. ^g After 18.5 h.

the solvent was evaporated to dryness and the residue was subjected to column chromatography on Sephadex LH-20 using MeOH/MeCN (7:3) as eluent. Only a center cut of the main band was collected, and the product was obtained from the concentrate upon standing. The recrystallization performed in MeCN/EtOH. Yield: 50%, 41.7 mg. Anal. Calcd for C₈₄H₇₂Cl₅N₁₂O₁₂Re₃Ru: C, 44.28; H, 3.19; N, 7.38. Found: C, 43.99; H, 3.44; N, 7.10. ESI-MS in MeCN (*m/z*): 738, [M – 2PF₆ – Cl + MeCN]³⁺; 1104, [M – 2PF₆]²⁺. ¹H NMR (DMSO-*d*₆) [δ in ppm (integration, multiplicity), assignment]: 8.87 and 8.83 (12H, d), 6 and 6'; 8.68 and 8.64 (12H, s), 4 and 4'; 7.61 and 7.57 (12H, d), 5 and 5'; 5.21 (3H, br), CH; 4.31 (12H, br), CH₂; 3.30 (18H, s), CH₃.

Results

Photocatalytic Reduction of CO₂. Good photocatalytic activities were obtained when the tetranuclear complex **RuRe₃** or the binuclear complex **d₂Ru–Re** was used in the reduction of CO₂ (Table 1). In both cases, carbon monoxide (formed catalytically) and a very small amount of dihydrogen were produced. No formic acid was observed in the reaction solution after the irradiation. The quantum yields of CO formation were 0.120 and 0.093 for **d₂Ru–Re** and **RuRe₃** respectively, using 480-nm monochromatic light at 1.54×10^{-6} einstein/min. Figure 2 shows the turnover numbers (TN_{CO}, mol of the CO produced/mol of the complex) versus the irradiation time. The bi- and tetranuclear photocatalysts respectively exhibited turnover numbers of 170 and 240 for CO formation after 16 h of light irradiation. A 1 mL reaction solution with **d₂Ru–Re** was added, after 7-h irradiation, to 10 mL of 1:1 solution of acetonitrile mixed with aqueous buffer (pH 1.8), and this solution was then subjected to column chromatography on SP-Sephadex C-25 using a 1:1 mixture of acetonitrile and aqueous buffer (pH 5.0, containing 20 mM NH₄PF₆). The main band was collected, and acetonitrile was evaporated. The precipitate was washed with water and analyzed by the ESI-MS spectrometer, with acetonitrile as eluent. Peaks attributable to the Cl⁻-substituted complex [(bpy)₂Ru(bpyC₃bpy)Re(CO)₃(MeCN)]³⁺, with which the acetonitrile ligand should coordinate during the post-treatments, were observed at *m/z* = 393, [M]³⁺, and 661, [M + PF₆]²⁺, with peaks attributed to the starting complex

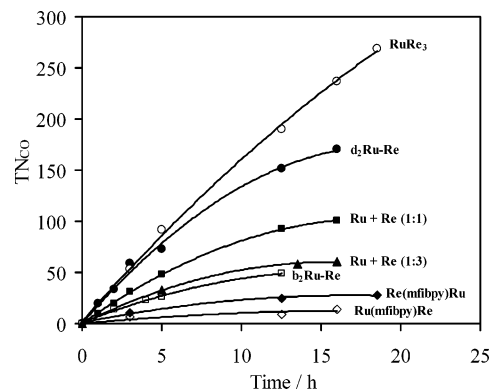


Figure 2. Turnover number for production of CO from CO₂ as a function of irradiation time. For selective excitation of the ruthenium moiety, solutions were irradiated at $\lambda \geq 500$ nm using a high-pressure Hg lamp, in a merry-go-round irradiation apparatus, combined with a uranyl glass and a K₂CrO₄ (30% w, *d* = 1 cm) solution filter. The concentration of the photocatalysts used is 0.05 mM, in a CO₂-saturated DMF/TEOA (5:1) solution containing 0.1 M of the sacrificial reagent BNAH.

d₂Ru–Re. Catalytic formation of CO continued after 7-h irradiation, as shown in Figure 2.

An equimolar mixed solution of [Ru(dmb)₃]²⁺ and [(dmb)Re(CO)₃Cl], which is a model of **d₂Ru–Re**, had a turnover number of 100 after 16-h irradiation, when it reached its plateau. In mixed solutions of the mononuclear complexes, an increase in the concentration of [(dmb)Re(CO)₃Cl] caused a decrease in TN_{CO}. For example, after 16-h irradiation of a solution containing 0.05 mM of [Ru(dmb)₃]²⁺ and 0.15 mM of [(dmb)Re(CO)₃Cl], a model of **RuRe₃**, TN_{CO} was only 61 on the basis of the [Ru(dmb)₃]²⁺ used (Figure 2). In the absence of [Ru(dmb)₃]²⁺, a mononuclear Re complex [(dmb)Re(CO)₃Cl] gave a turnover number of only ca. 15 under the same conditions except that 365-nm excitation was used. Without addition of the ruthenium complex, [Ru(dmb)₃]²⁺ did not itself show any photocatalytic activity for CO₂ reduction.

The photocatalytic abilities of the binuclear complexes with the mfiibpy bridging ligand, i.e., **Ru(mfiibpy)Re** and **Re(mfiibpy)Ru**, were much inferior to those with the bpyC₃-bpy ones **d₂Ru–Re** and **RuRe₃**. In the case where (CF₃)₂-bpy or bpy were used as peripheral ligands, the binuclear complexes also had poor photocatalytic ability, i.e., showing TN_{CO} of 3 and 50 respectively using **tfbRu–Re** and **b₂Ru–Re** (Figure 2).

Absorption and Emission Properties. Absorption and emission maxima, molar extinction coefficients, and emission lifetimes for the complexes are summarized in Table 2. Absorption and emission spectra of typical examples are shown in Figures 3 and 4. Absorption features appearing in the visible region at 365 and 400–550 nm correspond to spin-allowed ¹MLCT transitions initiated from the Re and Ru centers, respectively. The intense absorption band in the UV region (ca. 287 nm) is due to ligand-centered (π – π^*) transitions associated mainly with the polypyridine units.

In the bpyC₃bpy complexes, the spectra exhibited by the binuclear complexes match with a sum spectrum of the model complexes for each component unit, for example [Ru(dmb)₃]²⁺ and [(dmb)Re(CO)₃Cl]. As shown in Figure 3A, in the case of **d₂Ru–Re**, there was no detectable perturbation

Table 2. Spectroscopic and Photophysical Properties of the Ru and Re Complexes^a

complex	$\lambda_{\text{abs}}^b/\text{nm}$ ($10^{-3}\epsilon_{\text{max}}^c/\text{M}^{-1}\text{cm}^{-1}$)				
	$\pi-\pi^*$	MLCT	$\lambda_{\text{em}}^b/\text{nm}$ (298 K)	E_{00}^d/cm^{-1} (298 K)	τ^e/ns (298 K)
$\text{d}_2\text{Ru}-\text{Re}$	287 (94.5)	459 (14.9)	631	15 920	750
$\text{b}_2\text{Ru}-\text{Re}$	239 (42.3), 288 (89.7)	453 (14.1)	631	15 840	800
$\text{tfbRu}-\text{Re}$	242 (42.6), 296 (77.9)	478 (11.6)	671	14 870	560
$\text{Ru}(\text{mfibpy})\text{Re}$	248 (58.8), 282 (103)	442 (24.2)	646	15 530	930
$[(\text{mfibpy})\text{Ru}(\text{dmb})_2]^{2+}$	248 (47.8), 285 (96.9)	466 (18.2)	638	15 730	1520
$\text{Re}(\text{mfibpy})\text{Ru}$	248 (45.3), 286 (85.6)	457 (26.0)	637	15 780	1390
RuRe_3	291 (95.4) ^f	462 (12.7) ^e	638 ^e	15 920 ^e	860

^a The values were obtained in MeCN at room temperature unless otherwise noted. ^b Uncertainties in λ_{abs} and λ_{em} are ± 1 nm. ^c Estimated error in ϵ_{max} is $\pm 5\%$. ^d Estimated error in E_{00} is ± 30 cm^{-1} . ^e Uncertainty in lifetime values is $< 6\%$. ^f In DMF at room temperature.

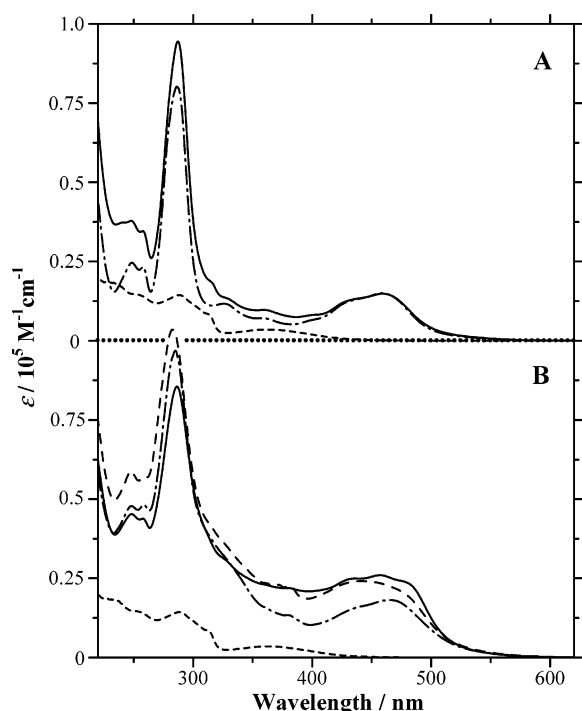


Figure 3. Room-temperature absorption spectra of metal complexes in MeCN: (A) $[(\text{dmb})\text{Re}(\text{CO})_3\text{Cl}]$ (dashed line), $[(\text{dmb})_2\text{Ru}(\text{bpyC}_3\text{bpy})](\text{PF}_6)_2$ (dotted–dashed line), $\text{d}_2\text{Ru}-\text{Re}$ (solid line); (B) $[(\text{dmb})_2\text{Ru}(\text{mfibpy})](\text{PF}_6)_2$ (dotted–dashed line), $\text{Ru}(\text{mfibpy})\text{Re}$ (dashed line), $\text{Re}(\text{mfibpy})\text{Ru}$ (solid line).

in these spectra, indicating that the electronic communication across the bridge is very weak. For $\text{tfbRu}-\text{Re}$, the MLCT absorption peaked at a longer wavelength (Table 2), showing clearly that as a result of the strong σ -withdrawing character of CF_3 substituents, the ligand π^* orbitals are stabilized and the lowest lying MLCT state is localized on the peripheral ligands, i.e., $(\text{CF}_3)_2\text{bpy}$. As for $\text{b}_2\text{Ru}-\text{Re}$, the lowest MLCT absorption could be assigned to either the bridge or peripheral ligands in view of the broad nature of the MLCT band.

In the mfibpy complexes, weak bands in the 360–380-nm range may also be assigned to the bridging ligand. In the binuclear complexes, the $^1\text{MLCT}$ absorption of the Re center seems to be obscured by these bands. The MLCT band shapes due to the Ru center were in all the mfibpy binuclear complexes different from that in the Ru mononuclear complex $[(\text{mfibpy})\text{Ru}(\text{dmb})_2]^{2+}$ (Figure 3B). The bridging ligand mfibpy is a fully π -conjugated system mediating strong electronic communication between the metal centers.

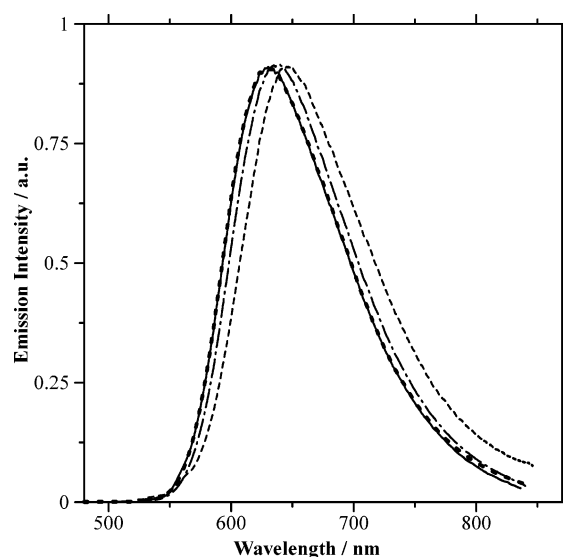


Figure 4. Corrected emission spectra of $\text{Ru}(\text{mfibpy})\text{Re}$ (dashed line), $[(\text{mfibpy})\text{Ru}(\text{dmb})_2](\text{PF}_6)_2$ (dotted–dashed line), and $[(\text{dmb})_2\text{Ru}(\text{bpyC}_3\text{bpy})](\text{PF}_6)_2$ (solid line) at room temperature in MeCN solution. For comparison, the spectrum of $[\text{Ru}(\text{dmb})_3](\text{PF}_6)_2$ (dotted line) is also superimposed on the solid line ($\lambda_{\text{ex}} = 460$ nm).

Therefore, in the binuclear complexes, new molecular orbital coefficients contribute in constructing the MLCT absorption band.

The luminescence of the binuclear complexes with bpyC_3bpy can be described using an energy diagram on the basis of superimposing the lowest excited states of the Ru and Re moieties. An efficient quenching of emission at wavelengths shorter than 600 nm, which comes predominantly from the Re moiety, and enhancement of emission intensity at wavelengths longer than 600 nm, which is from the Ru moiety, were observed. It follows that the emission spectra of the binuclear complex $\text{d}_2\text{Ru}-\text{Re}$ are identical with the corresponding Ru mononuclear $[(\text{dmb})_2\text{Ru}(\text{bpyC}_3\text{bpy})]^{2+}$, as depicted in Figure 4. We therefore conclude that an inter-component energy transfer occurs from an upper lying Re excited state of the $[(\text{bpyC}_3\text{bpy})\text{Re}(\text{CO})_3\text{Cl}]$ moiety to the lower lying Ru $^3\text{MLCT}$ excited state of the $[(\text{dmb})_2\text{Ru}(\text{bpyC}_3\text{bpy})]$ subunit in these supramolecular complexes. In the cases of $\text{tfbRu}-\text{Re}$ and $\text{b}_2\text{Ru}-\text{Re}$, similar energy transfer from the Re moiety to the Ru was observed. A detailed study of the energy transfer mechanism and rates for $\text{b}_2\text{Ru}-\text{Re}$ has been addressed previously.¹²

In the binuclear complexes with mfibpy , efficient quenching of the Re excited state was also observed. However, as

Table 3. Redox Potentials of Ru and Re Complexes (V)^a

compd	$E_{1/2}(\text{oxdn})$	$E_{1/2}(\text{redn})$	$E_{1/2}^*(\text{redn})$
[Ru(dmb) ₃] ²⁺ ^b	+0.74	-1.77, -1.96, -2.22	+0.20
[(dmb) ₂ Ru(bpyC ₃ bpy)] ²⁺	+0.77	-1.76, -1.95, -2.22, -2.55	
[(dmb)Re(CO) ₃ Cl]	+0.92	-1.78, -1.98, -2.15, -2.3	
[(mfibpy)Re(CO) ₃ Cl]	+0.90	-1.41, ^c -1.80, -2.28, -2.54	
[(mfibpy)Ru(dmb) ₂] ²⁺	+0.81	-1.28, -1.50, -1.82, -2.03	+0.67
d ₂ Ru–Re	+0.75, +0.94	-1.77, ^c -1.97, -2.24	+0.20
b ₂ Ru–Re	+0.85, +1.13	-1.73, -1.87, -1.96, -2.01	+0.23
tfbRu–Re	+0.94, +1.14	-1.23, -1.41, -1.76, -1.87	+0.61
Ru(mfibpy)Re	+0.89, +1.04	-1.10, -1.33, -1.65, -1.80	+0.83
Re(mfibpy)Ru	+0.81, +1.01	-1.10, -1.28, -1.50, -1.63	+0.86
RuRe₃ ^b	+0.77, +0.91	-1.80, ^d -2.04, -2.34	+0.17

^a The values were obtained at room temperature and in MeCN solutions containing 0.1 M TBAH. All $E_{1/2}$ values are referenced to the $E_{1/2}$ of the Ag/AgNO₃ redox couple (0.32 V vs SCE in MeCN); for comparison, the redox potentials of [Ru(dmb)₃]²⁺ are also presented. ^b In DMF (0.1 M TBAH). ^c Two-electron reduction. ^d Broad but very close to a three-electron reduction.

a result of strong electronic communication between the metal centers in the **Ru(mfibpy)Re** complex, we found that the luminescence band maximum was at lower energy (646 nm) for the binuclear complexes than for the mononuclear complex (Figure 4). This behavior is due to a stabilizing effect, as a result of coordination to the second metal center, on the π^* level of the imidazolyl motif of the bridging ligand mfibpy that is involved in the MLCT excited-state responsible for the luminescence.

We conclude that the lowest lying luminescent level is Ru-centered in all of the supramolecular complexes. Also, since we performed a selective excitation of the Ru-based chromophore at $\lambda_{\text{ex}} = 480$ nm in quantum yield measurements, or $\lambda_{\text{ex}} \geq 500$ nm in photocatalytic reduction of CO₂, we consider only reductive quenching of the Ru ³MLCT excited state in the following sections.

Electrochemical Properties. The electrochemical behavior of the complexes is summarized in Table 3. The redox processes of the individual components were maintained in all of the bpyC₃bpy complexes. The cyclic voltammograms of the complexes were consistent with metal-based oxidation and several ligand-based reductions. We can assign the first reduction wave to the peripheral ligands in **tfbRu–Re** (at -1.23 V vs Ag/Ag⁺ in MeCN containing 0.1 M TBAH) by analogy with [((CF₃)₂bpy)₂Ru(dmb)]²⁺ (-1.21 V). In the case of **d₂Ru–Re**, the first reduction wave at -1.77 V corresponds to a two-electron reduction. At this potential the Ru and Re sites of the bpyC₃bpy bridging ligand should both be reduced, since the first reduction wave in the model complexes [Ru(dmb)₃]²⁺ and [(dmb)Re(CO)₃Cl] were observed at -1.77 and -1.78 V, respectively. This implies that there is no strong electronic interaction between either end of the bridging ligand in the OER species of **d₂Ru–Re**. In the case of **b₂Ru–Re**, the first two reduction waves (at ca. -1.73 and -1.87 V) are poorly resolved so that assignment is rather difficult. Since the first reduction in the model complexes [(bpy)₂Ru(dmb)]²⁺ and [(dmb)Re(CO)₃Cl] happens at -1.68 and -1.78 V, respectively, these could be assigned to sequential reductions of the bpy ligand of the ruthenium site and the bridging ligand on the rhenium end.

In line with these results and on the basis of the known

correlation between electrochemical and spectroscopic properties,^{3,6,20} the lowest lying MLCT state in **tfbRu–Re** is expected to reside on the peripheral (CF₃)₂bpy ligand, due to the strong σ -withdrawing character of the CF₃ substituents.¹⁹ This is responsible for a shift of 0.40 V in the first reduction potential of **tfbRu–Re** compared to **b₂Ru–Re**. In the case of **d₂Ru–Re**, a bridging ligand localization of the lowest lying MLCT state is expected.

By comparing the first reduction potentials observed for mononuclear complexes with mfibpy ligand [(mfibpy)Re(CO)₃Cl] and [(dmb)₂Ru(mfibpy)]²⁺ at -1.44 and -1.29 V, respectively, with those of corresponding reference complexes of [(dmb)Re(CO)₃Cl] and [Ru(dmb)₃]²⁺, we can assign the first reduction wave to the bridging ligand mfibpy. Introduction of the second metal into the complex shifted the potentials anodically to ca. -1.10 V in both the **Ru(mfibpy)Re** and **Re(mfibpy)Ru** binuclear complexes. This is due to stabilization of the π^* LUMO localized on the mfibpy. The inequivalence of the binding sites in mfibpy is indicated by comparing the metal oxidation potentials in two binuclear complexes as well as their respective mononuclear complexes [(mfibpy)Re(CO)₃Cl] and [(mfibpy)Ru(dmb)₂]²⁺. For **Ru(mfibpy)Re**, the first oxidation wave occurred at a potential more positive (+0.89 V) than those of the Ru^{3+/2+} couple in **Re(mfibpy)Ru** and [(mfibpy)Ru(dmb)₂]²⁺ (both at +0.81 V). This clearly shows that the Ru in **Ru(mfibpy)Re** is coordinated to the phenanthroline site of the mfibpy, which has a higher π acceptability than the other bpy site.⁶ In [(mfibpy)Re(CO)₃Cl], the Re^{2+/+} wave is at a potential similar to that in [(dmb)Re(CO)₃Cl]. However, in **Ru(mfibpy)Re** and **Re(mfibpy)Ru**, the Re oxidation wave was shifted positively by up to 140 mV due to electrostatic interaction between the metal centers. It is apparent that the mfibpy ligand allows substantial electronic communication across the bridge.

Discussion

We have successfully synthesized a number of bi- and tetranuclear supramolecular complexes in the development of CO₂ reduction photocatalysts. These are constructed with an photosensitizer part, using the ruthenium(II) bpy-type complex, and a catalyst part based on the rhenium(I) complexes. Several kinds of peripheral and bridging ligands were used in the synthesis of the supramolecular structure, as shown in Figure 1. The photocatalytic activities of these supramolecules were strongly influenced by the choice of both the peripheral and the bridging ligands. Interesting results were obtained using the bpyC₃bpy complexes **d₂Ru–Re** with the dmb peripheral ligands and **RuRe₃** as photocatalyst. Features include high selectivity of production of CO over H₂, relatively high quantum yields, and a surprisingly large turnover number for CO formation. In contrast, the binuclear complexes with the mfibpy bridging ligand or the (CF₃)₂bpy peripheral ligands had much lower photocata-

(20) (a) Vlcek, A. A.; Dostworth, E. S.; Pietro, W. J.; Lever, A. B. P. *Inorg. Chem.* **1995**, *34*, 1906. (b) Barigelletti, F.; Juris, A.; Balzani, V.; Belser, P.; von Zelewsky, A. *Inorg. Chem.* **1987**, *26*, 4115.

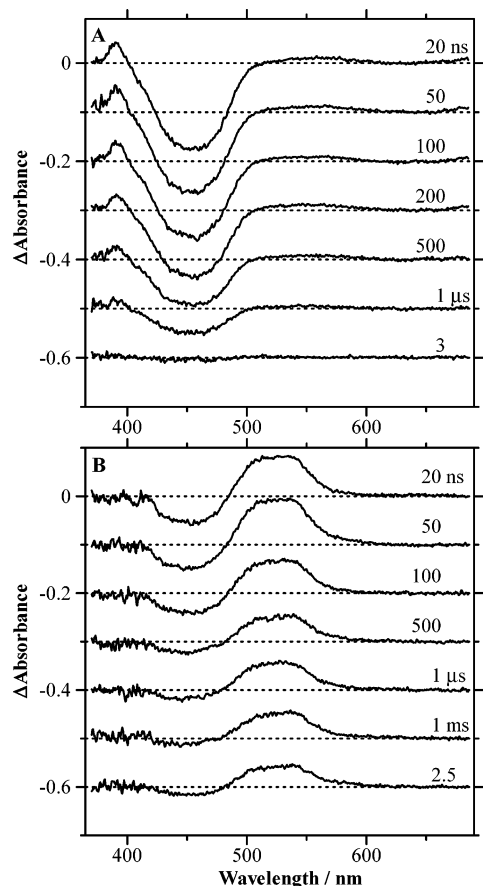
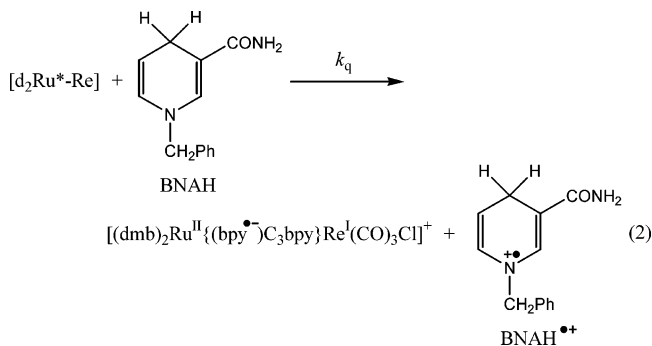
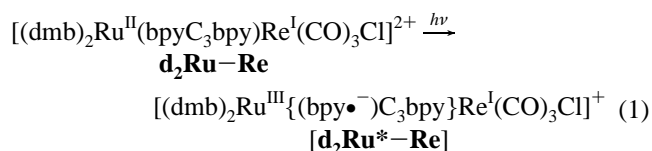


Figure 5. Time-resolved transient absorption spectra of **d₂Ru–Re** (A) without and (B) with the sacrificial reagent ([BNAH] = 0.1 M) in argon-saturated DMF at room temperature ($\lambda_{\text{ex}} = 532$ nm).

lytic activity or none. Even replacement of the dmb ligands by bpy (**b₂Ru–Re**) caused a dramatic decrease in TN_{CO} , as shown in Figure 2. Why are the photocatalytic abilities of these supramolecules so sensitive to the ligands? The answer will provide important information for designing new supramolecules with improved catalytic ability.

Mechanism of Photocatalytic Reaction. The $^3\text{MLCT}$ excited state of the ruthenium moiety in all of Ru–Re supramolecular complexes was efficiently quenched by BNAH when the excitation wavelength corresponded to the absorption regions of the Ru moiety ($\lambda \geq 470$ nm). Table 1 shows the quenching rates (k_q), calculated from linear Stern–Volmer plots and lifetimes of the luminescence from the $^3\text{MLCT}$ excited state, and the quenched fractions of the $^3\text{MLCT}$ excited state (η_q), obtained in the presence of 0.1 M BNAH. The quenching process should be reductive, since generation of the one-electron-reduced (OER) species of the Ru moiety was confirmed by transient absorption spectroscopy. As an example, Figure 5 shows the transient absorption (TA) spectra of the **d₂Ru–Re** in DMF. In the absence of BNAH, TA spectra showed positive absorption at $\lambda < 400$ nm and strong bleaching centered at 460 nm, which is typical of the formation of the $^3\text{MLCT}$ excited state of Ru(II) polypyridine complexes with characteristic transitions within the polypyridine radical anion and the disappearance of the ground-state MLCT band.²¹ The absorption decayed completely via first-order kinetics ($k = 1.1 \times 10^6 \text{ s}^{-1}$),

consistent with the decay rate of the emission (Figure 5A). In the presence of BNAH, new spectral features developed in the TA spectra: depletion of the ground-state MLCT band at 455 nm and an intense absorption at 480–580 nm, as shown in Figure 5B. These spectral features were also observed in a spectrum obtained from the continuous photolysis ($\lambda_{\text{ex}} = 480$ nm) of a DMF solution containing $[\text{Ru}(\text{dmb})_3]^{2+}$ and BNAH (0.1 M) under argon atmosphere (Figure 6A). These spectra are very similar to that of $[\text{Ru}(\text{bpy})_2(\text{bpy}^{\bullet-})]^+$ obtained by controlled electrochemical reduction of $[\text{Ru}(\text{bpy})_3]^{2+}$ in dimethyl sulfoxide.²² Therefore, it is very likely that the added electron resides on the Ru-bound bpy end of the bridging ligand bpyC_3bpy and the charge distribution is $[(\text{dmb})_2\text{Ru}^{\text{II}}\{(\text{bpy}^{\bullet-})\text{C}_3\text{bpy}\}\text{Re}^{\text{I}}(\text{CO})_3\text{Cl}]^+$, which is probably equilibrated with $[(\text{dmb}^{\bullet-})(\text{dmb})\text{Ru}^{\text{II}}(\text{bpyC}_3\text{bpy})\text{Re}^{\text{I}}(\text{CO})_3\text{Cl}]^+$. The OER species of the Re moiety was not detected in a time-resolved IR spectrum obtained immediately after a laser flash into a DMF solution of **d₂Ru–Re** containing BNAH and TEA.^{23,24} From these results, initiation processes of the **d₂Ru–Re**-photocatalyzed CO_2 reduction can be deduced, as in eqs 1 and 2.



The other additive TEOA could not quench the $^3\text{MLCT}$ excited state of $[\text{d}_2\text{Ru}^*-\text{Re}]$ at all, while it has been often

- (21) (a) Braterman, P. S.; Harriman, A.; Heath, G. A.; Yellowless, L. J. *J. Chem. Soc., Dalton Trans.* **1983**, 1801. (b) Gholamkhash, B.; Nozaki, K.; Ohno, T. *J. Phys. Chem. B* **1997**, *101*, 9010.
- (22) Heath, G. A.; Yellowless, L. J. *J. Chem. Soc., Chem. Commun.* **1981**, *1*, 287.
- (23) The ν_{CO} bands in the OER species of the Re complex $[\text{Re}(\text{bpy}^{\bullet-})(\text{CO})_3\text{P}(\text{OEt})_3]^+$ were observed at $\sim 50 \text{ cm}^{-1}$ lower energy than those of the original form $[\text{Re}(\text{bpy})(\text{CO})_3\text{P}(\text{OEt})_3]^+$, because of the stronger π -back-donation from the Re(I) $d\pi$ orbital to the ligand π^* one; see for example: Ishitani, O.; George, M. W.; Ibusuki, T.; Johnson, F. P. A.; Koike, K.; Nozaki, K.; Pac, C.; Turner, J. J.; Westwell, J. R. *Inorg. Chem.* **1994**, *33*, 4712.
- (24) Time-resolved IR spectroscopy has been applied to several issues related to excited states and electronic structure in polypyridine complexes containing carbonyl ligands; see for example: (a) Dattelbaum, D. M.; Omberg, K. M.; Schoonover, J. R.; Martin, R. L.; Meyer, T. J. *Inorg. Chem.* **2002**, *41*, 6071. (b) Koike, K.; Okoshi, N.; Hori, H.; Takeuchi, K.; Ishitani, O.; Tsubaki, H.; Clark, I. P.; George, M. W.; Johnson, F. P. A.; Turner, J. J. *J. Am. Chem. Soc.* **2002**, *124*, 11448. (c) George, M. W.; Poliakov, M.; Turner, J. J. *Analyst* **1994**, *119*, 551.

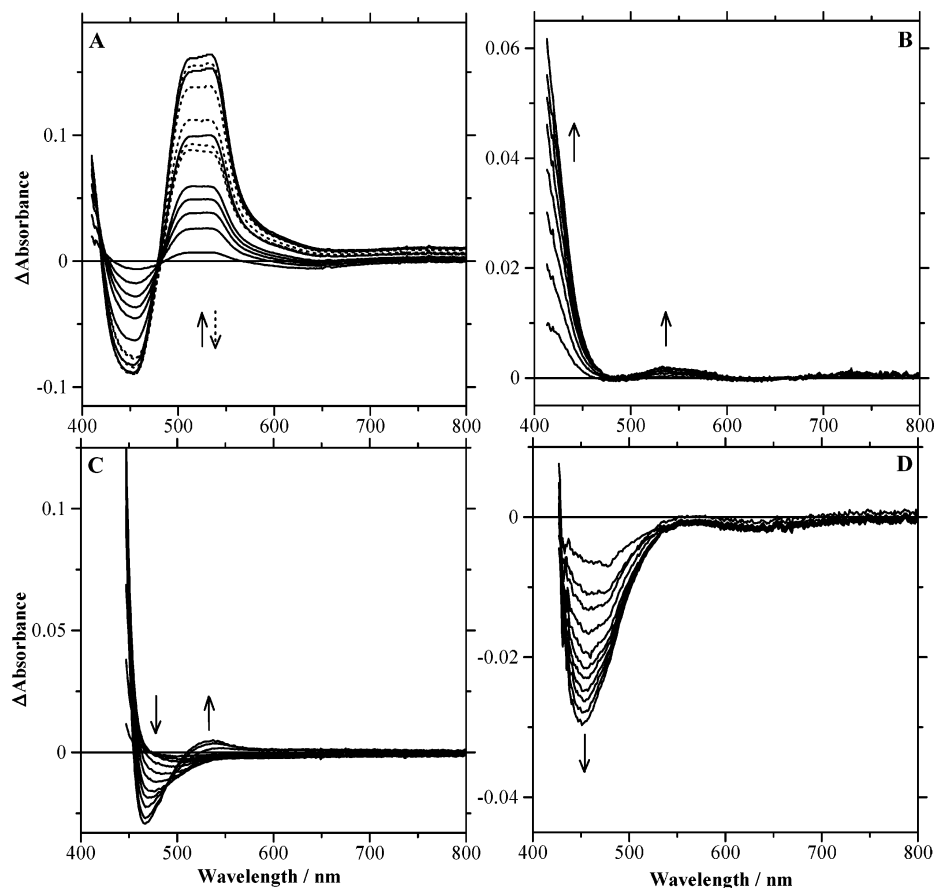
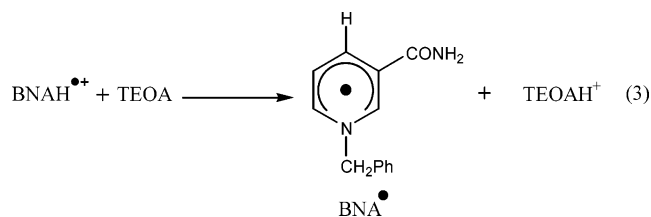


Figure 6. Steady-state measurement of the change in absorption spectra of argon-saturated DMF/TEOA/BNAH (0.1 M) solutions of (A) $[\text{Ru}(\text{dmb})_3](\text{PF}_6)_2$ ($\lambda_{\text{ex}} = 480$ nm, 15 s intervals), (B) $[(\text{dmb})\text{Re}(\text{CO})_3\text{Cl}]$ ($\lambda_{\text{ex}} = 365$ nm, 5 min intervals), and (C) $\text{d}_2\text{Ru}-\text{Re}$ ($\lambda_{\text{ex}} = 480$ nm, 10 s intervals). (D) is the same as (C) except that the solution is saturated with CO_2 .

used as a sacrificial electron donor in metallic systems.²⁵ Lack of TEOA, however, slowed the photocatalytic CO_2 reduction. It has been reported that deprotonation of $\text{BNAH}\cdot^+$ is accelerated in the presence of the base.²⁶ TEOA should therefore play a role as a base to inhibit back electron transfer from $[(\text{dmb})_2\text{Ru}^{\text{II}}\{(\text{bpy}\cdot^-)\text{C}_3\text{bpy}\}\text{Re}^{\text{I}}(\text{CO})_3\text{Cl}]^+$ to $\text{BNAH}\cdot^+$, as in eq 3. Following light irradiation, the oxidized dimers



(25) (a) Sun, H.; Hoffman, M. Z. *J. Phys. Chem.* **1994**, *98*, 11719. (b) Neshvad, G.; Hoffman, M. Z.; Mulazzani, Q. G.; Venturi, M.; Ciano, M.; D'Angelantonio, M. *J. Phys. Chem.* **1989**, *93*, 6080. (c) Sun, H.; Hoffman, M. Z. *J. Phys. Chem.* **1989**, *93*, 2445. (d) Kalyanasundaram, K., Grätzel, M., Eds. *Photosensitization and Photocatalysis using Inorganic and Organometallic Compounds*; Kluwer Academic Publishers: Dordrecht, The Netherlands, 1993; Vol. 14. (e) Canon, M., Ed. *Homogeneous photocatalysis*; John Wiley & Sons Ltd.: West Sussex, U.K., 1997. (f) Hori, H.; Johnson, F. P. A.; Koike, K.; Takeuchi, K.; Ibusuki, T.; Ishitani, O. *J. Chem. Soc., Dalton Trans.* **1997**, 1019. (g) Hori, H.; Ishizuka, J.; Koike, K.; Takeuchi, K.; Ibusuki, T.; Ishitani, O. *Chem. Lett.* **1998**, 1249. (h) Hori, H.; Koike, K.; Takeuchi, K.; Ishitani, O. *Chem. Lett.* **2000**, 376.

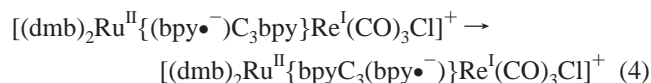
(26) Pac, C.; Miyauchi, Y.; Ishitani, O.; Ihama, M.; Yasuda, M.; Sakurai, H. *J. Org. Chem.* **1984**, *49*, 26.

of BNAH, produced by coupling of $\text{BNA}\cdot$, were confirmed by ESI-MS measurement as in $[(\text{BNA})_2]^+$ ($m/z = 425$).

As seen in Figure 5B, transient features due to the OER species, i.e., $[(\text{dmb})_2\text{Ru}^{\text{II}}\{(\text{bpy}\cdot^-)\text{C}_3\text{bpy}\}\text{Re}^{\text{I}}(\text{CO})_3\text{Cl}]^+$, lasted up to 2.5 ms. This experiment was followed by continuous photolysis under argon or CO_2 atmosphere. Figure 6B,C show absorption spectra changes obtained for the continuous photolysis under argon of a DMF solution containing either $[(\text{dmb})\text{Re}(\text{CO})_3\text{Cl}]$ or $\text{d}_2\text{Ru}-\text{Re}$ in the presence of both BNAH and TEOA. In the former ($\lambda_{\text{ex}} = 365$ nm), the OER species $[(\text{dmb}\cdot^-)\text{Re}^{\text{I}}(\text{CO})_3\text{Cl}]$ became detectable within several minutes from its weak but distinct absorption around 530 nm.^{8,23,27} In the latter, 530-nm absorption was also detected within a similar time scale. In this case, although depletion of the ground-state MLCT band was observed, the Δ absorbance had a much smaller absolute value than for $[\text{Ru}(\text{dmb})_3]^{2+}$ (Figure 6A), for which the spectrum corresponds to the OER species of Ru moiety. Since the spectra (Figure 6A,C) are not similar as expected if the same species were involved, the depletion is attributed to decomposition of a small amount of the Ru moiety. These data strongly suggest that the absorption around 530 nm observed during continuous irradiation of $\text{d}_2\text{Ru}-\text{Re}$ (Figure 6C) is due to

(27) (a) Kalyanasundaram, K. *J. Chem. Soc., Faraday Trans. 2* **1986**, *82*, 2401. (b) Kutal, C.; Weber, M. A.; Ferraudi, G.; Geiger, D. *Organometallics* **1985**, *4*, 2161. (c) Kutal, C.; Corbin, A. J.; Ferraudi, G. *Organometallics* **1987**, *6*, 553.

the OER species of the Re moiety, i.e., $[(\text{dmb})_2\text{Ru}^{\text{II}}\{\text{bpyC}_3\text{-}(\text{bpy}\bullet^-)\}\text{Re}^{\text{I}}(\text{CO})_3\text{Cl}]^+$. Since the excitation wavelength of 480 nm or longer cannot excite the Re moiety, appearance of the reduced Re moiety must be interpreted in terms of intramolecular electron transfer from the reduced Ru-bound bpy to the Re site, as shown in eq 4.



This intramolecular electron transfer in the ground state should proceed at an exchange rate ($\Delta G = 0$), since the first reduction potential of the Re moiety ($E_{1/2} = -1.77$ V) is equal to that of the Ru moiety (Table 3). It has been reported that the OER of $[(\text{bpy})\text{Re}(\text{CO})_3\text{Cl}]$ reacts with CO_2 via a ligand loss process within several seconds to give CO .²⁸ It is reasonable to suppose that $[(\text{dmb})_2\text{Ru}^{\text{II}}\{\text{bpyC}_3(\text{bpy}\bullet^-)\}\text{Re}^{\text{I}}(\text{CO})_3\text{Cl}]^+$ reacts with CO_2 via Cl^- loss at a similar rate. ESI-MS analysis of the reaction products showed that the Cl^- ligand in the diad was partially released during the photocatalytic reaction. It follows that reduction of CO_2 with the OER species of the Re moiety is the rate-determining process in the photocatalytic reduction of CO_2 by $\mathbf{d}_2\text{Ru}-\text{Re}$. This is an important reason $\mathbf{d}_2\text{Ru}-\text{Re}$, and probably \mathbf{RuRe}_3 , can act as efficient supramolecular photocatalysts for CO_2 reduction, even though intramolecular electron transfer from the photosensitizer Ru moiety to the catalyst Re moiety is relatively slow. We are unable to follow reactions occurring on time scales greater than 2.5 ms by TA or greater than 100 ms by time-resolved IR spectroscopies,²³ so that we can state only that intramolecular electron transfer is a relatively slow process that takes several hundred milliseconds to a second.

The following section discusses the molecular architecture necessary for constructing supramolecular photocatalysts using both the information described above and a comparison with the results of other systems.

Architectural Requirement. A detailed comparison of the photocatalytic activities of the binuclear complexes with the bpyC_3bpy bridging ligand, i.e., $\mathbf{tfbRu}-\text{Re}$, $\mathbf{b}_2\text{Ru}-\text{Re}$, and $\mathbf{d}_2\text{Ru}-\text{Re}$, clearly shows that, to design a supramolecule that efficiently photocatalyzes reduction of CO_2 , electron transfer from the photosensitizer Ru site to the catalyst Re site must not be endothermic. In the cases of $\mathbf{tfbRu}-\text{Re}$ and $\mathbf{b}_2\text{Ru}-\text{Re}$, the production of OER species of the Re moiety is not favored energetically, because the intramolecular electron transfer is endothermic ($\Delta G = +0.55$ and $+0.05$ eV, respectively). In the photocatalytic reaction using $\mathbf{tfbRu}-\text{Re}$, the OER species $\{[(\text{CF}_3)_2\text{bpy}\}\{(\text{CF}_3)_2\text{bpy}\bullet^-\}\text{Ru}^{\text{II}}(\text{bpyC}_3\text{bpy})\text{Re}^{\text{I}}(\text{CO})_3\text{Cl}\}^+$ was indeed accumulated in the solution, but only a small amount of CO was produced. Although the difference in the endothermicity of the electron transfer between $\mathbf{b}_2\text{Ru}-\text{Re}$ and $\mathbf{d}_2\text{Ru}-\text{Re}$ is very small (only

+0.05 eV), the photocatalytic activity of $\mathbf{b}_2\text{Ru}-\text{Re}$ is much lower than that of $\mathbf{d}_2\text{Ru}-\text{Re}$. Therefore, as well as the energetic aspect, electron localization on the bridging ligand seems to be a further decisive factor in view of the required function of the electron transfer between the subunits.

The nature of the bridging ligand itself plays a fundamental role in defining the electrochemical and spectroscopic properties of the supramolecular systems. For $\mathbf{Ru}(\text{mfibpy})-\text{Re}$ and $\mathbf{Re}(\text{mfibpy})\text{Ru}$, although the requirement of bridging-ligand localization of the electron is satisfied, their photocatalytic abilities are low. Estimation of the free energy change is difficult in these binuclear complexes. We can assume that, in the case of $\mathbf{Ru}(\text{mfibpy})\text{Re}$, the electron is mainly localized on the Ru end of the bridging ligand, because the energy level of the π^* orbital on the phenanthroline–imidazolyl motif of mfibpy is lower than that on the bpy one coordinating to the Re. It follows that the low electron density on the catalytic Re site in the OER species must be a principal reason for the low photocatalytic activity of $\mathbf{Ru}(\text{mfibpy})\text{Re}$. In the case of $\mathbf{Re}(\text{mfibpy})\text{Ru}$, in contrast, electron localization must be on the Re site, which would give rise to its good photocatalysis. We have reported that photocatalyses of the mononuclear complexes $\text{fac}-[\text{Re}(\text{LL})(\text{CO})_3(\text{PR}_3)]^+$, where LL and R are respectively a diimine ligand and an alkyl group, depend strongly on their reduction potentials $E_{1/2}^{\text{red}}(\text{LL}/\text{LL}\bullet^-)$, and an efficient photocatalytic reduction of CO_2 requires $E_{1/2}^{\text{red}}(\text{LL}/\text{LL}\bullet^-) < -1.41$ V vs Ag/Ag^+ .^{8c} In view of the wide conjugation of the mfibpy and the strong electronic communication across the bridging ligand, the reducing power of the OER species ($E_{1/2}^{\text{red}} = -1.1$ V vs Ag/Ag^+) should be insufficient for efficient reduction of CO_2 under these conditions.

The strong electronic communication between the photosensitizer moiety and the catalyst moiety through the bridging ligand lessens the photocatalytic activity even though it accelerates the electron transfer between them. This fact should be an important general guide for constructing supramolecular systems to act as photocatalyst in CO_2 reduction. Electron transfer must occur from the reduced photosensitizer to the catalyst site, but this does not need to be a rapid process. This is because the following step, i.e., reaction of the OER species of the catalyst site with CO_2 , is usually slower.^{8c,28,29} In the case of the good photocatalyst $\mathbf{d}_2\text{Ru}-\text{Re}$, for example, the electron transfer proceeded at a time scale of several hundred milliseconds to seconds. The reducing power of the OER species of the catalyst site must be maintained as strong as possible, because it is the dominating factor determining the overall reaction rate of the OER species with CO_2 . Therefore, widely conjugated bridging ligands are not suitable for supramolecular photocatalysts of CO_2 reduction, since their π^* energy levels are lower than those of the corresponding nonconjugated ligands.

The formation of CO requires injection of one more electron into the reaction product(s) of the OER species with CO_2 (CO_2 adduct). Participation of $\text{BNA}\bullet$ is unlikely in view

(28) (a) Johnson, F. P. A.; George, M. W.; Hartle, F.; Turner, J. J. *Organometallics* **1996**, *15*, 3374. (b) Christensen, P.; Hamnett, A.; Muir, A. V. G.; Timney, J. A. *J. Chem. Soc., Dalton Trans.* **1992**, 1455. (c) Sullivan, P.; Bolinger, C. M.; Conrad, D.; Vining, W. J.; Meyer, T. J. *J. Chem. Soc., Chem. Commun.* **1985**, 1414.

(29) Hayashi, Y.; Kita, S.; Brunschwig, B. S.; Fujita, E. *J. Am. Chem. Soc.* **2003**, *125*, 11976 and references therein.

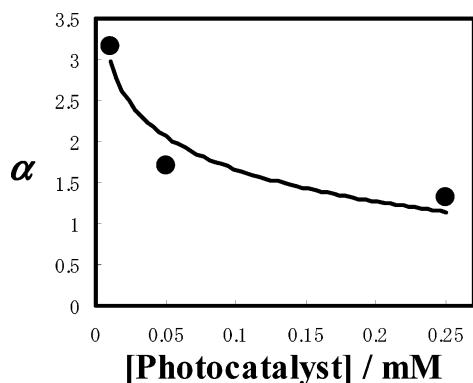


Figure 7. Concentration dependence of the relative TN_{CO} in the binuclear complex of d_2Ru-Re with respect to a 1:1 mixture of $[Ru(dmb)_3]^{2+}$ and $[(dmb)Re(CO)_3Cl]$ ($\alpha = TN_{CO}(bi)/TN_{CO}(mono's)$).

of its rapid dimerization to give BNA_2 's,³⁰ which were detected in the solutions after the photocatalytic reactions. The possible candidates are therefore the OER of the Ru moiety produced by second photochemical electron transfer from another $BNAH$ or another OER species of the starting complex. Figure 7 shows the concentration dependence of the relative TN_{CO} in the binuclear complex of d_2Ru-Re with respect to 1:1 mixture of mononuclear complexes, $[Ru(dmb)_3]^{2+}$ and $[(dmb)Re(CO)_3Cl]$, where $\alpha = TN_{CO}(bi)/TN_{CO}(mono's)$. At progressively lower concentrations, the binuclear system gained in superiority over the mixed mononuclear one. The proximity effect between the Ru and Re moiety in the supramolecule probably suppresses decomposition of the CO_2 adduct prior to injection of the second electron. A more dramatic proximity effect was observed by comparing $RuRe_3$ with a 1:3 mixture of $[Ru-$

$(dmb)_3]^{2+}$ and $[(dmb)Re(CO)_3Cl]$, as shown in Figure 2. Moreover, the lower TN_{CO} observed for the 1:3 mixture than the 1:1 mixture suggests that, in the mixed mononuclear system, the greater probability of capturing an electron from the OER species of $[Ru(dmb\bullet^-)(dmb)_2]^{2+}$ by $[(dmb)Re(CO)_3Cl]$ hampers the second electron transfer to the already formed CO_2 adduct. In the supramolecular system $RuRe_3$, no such decrease in TN_{CO} was observed, probably because the Ru moiety is always close to the CO_2 adduct, which could have greater oxidation power than the other Re moieties.

Conclusion

Enhancement of the photocatalytic response to light in the visible region is achieved by fabricating supramolecules featuring covalently linked ruthenium and rhenium moieties. The greatly improved photocatalytic activity in the case of the tetranuclear complex $RuRe_3$ and the binuclear complex d_2Ru-Re is attributed to intramolecular electron transfer, from the OER species $[(dmb)_2Ru^{II}\{(bpy)\bullet^-C_3bpy\}Re^I(CO)_3Cl]^+$ produced following the selective excitation and subsequent reductive quenching of the Ru 3MLCT excited state, to the Re moiety.

These results provide new information on the electrochemical and structural requirements needed to build supramolecular metal complexes which can be used as an efficient photocatalyst for CO_2 reduction. Future studies will focus on the design and application of new multinuclear metal complexes.

Acknowledgment. We thank Prof. Shigero Oishi (Kitasato University), who carried out the TRIR measurements. B.G. gratefully acknowledges the Research Institute of Innovative Technology for the Earth for a research fellowship. This work was partly supported by the RITE and CREST, JST.

IC048779R

(30) Pac, C.; Kaseda, S.; Ishii, K.; Yanagida, S.; Ishitani, O. In *Photochemical Processes in Organized Molecular Systems*; Honda, K., Kitamura, M., Masuhara, H., Ikeda, T., Sisido, M., Winnik, M. A., Eds.; Elsevier: Amsterdam, 1991; pp 177–186.